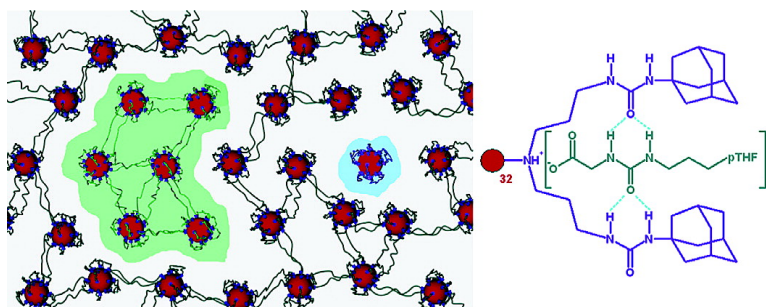


Dendrimer-Based Transient Supramolecular Networks

Ron M. Versteegen, D. J. M. van Beek, Rint P. Sijbesma,
 Dimitris Vlassopoulos, George Fytas, and E. W. Meijer

J. Am. Chem. Soc., **2005**, 127 (40), 13862-13868 • DOI: 10.1021/ja051775g • Publication Date (Web): 17 September 2005

Downloaded from <http://pubs.acs.org> on March 25, 2009



More About This Article

Additional resources and features associated with this article are available within the HTML version:

- Supporting Information
- Links to the 5 articles that cite this article, as of the time of this article download
- Access to high resolution figures
- Links to articles and content related to this article
- Copyright permission to reproduce figures and/or text from this article

[View the Full Text HTML](#)

Dendrimer-Based Transient Supramolecular Networks

Ron M. Versteegen,[†] D. J. M. van Beek,^{†,‡} Rint P. Sijbesma,[†]
Dimitris Vlassopoulos,[‡] George Fytas,^{‡,§} and E. W. Meijer^{*,†}

Contribution from the Laboratory of Macromolecular and Organic Chemistry, Eindhoven University of Technology, P.O. Box 513, 5600 MB Eindhoven, The Netherlands, Department of Materials Science and Technology, University of Crete and IESL/FORTH, P.O. Box 1527, 71110 Heraklion, Greece, and Max-Planck Institute for Polymer Research, P.O. Box 3148, 55128 Mainz, Germany

Received March 21, 2005; Revised Manuscript Received August 15, 2005; E-mail: e.w.meijer@tue.nl

Abstract: Association of a 16-fold excess of a monodisperse telechelic oligo(THF) ($M_w = 1270$ g/mol) containing two end groups that selectively bind to the 32 binding sites of a fifth generation dendritic host ($M_w = 18\,511$ g/mol and radius $R_h = 2.4$ nm) results in the formation of reversible and dynamic supramolecular complexes. The structure of these complexes in solution depends strongly on the concentration. At low concentration, the two end groups of one guest are proposed to complex to the same host, and flowerlike structures are formed with a radius of $R_h = 3.7$ nm. At higher concentrations, both end groups of one guest are complexed to different hosts, forming a bridge between them. This gives rise to the formation of larger associates, and eventually to a transient supramolecular network. Dynamic light scattering unequivocally showed that three distinct relaxation processes, associated with the proposed structures, are present in this system. In addition to the dynamics related to the flowerlike (fast) and the transient network structures (slow), an intermediate dynamic process is attributed to the cooperative motion of a few (~ 6) connected flowerlike structures. Rheological data elucidate the nature of the intermittent network responsible for the slowest process. A monofunctional guest, not capable of forming a network structure, was used as a reference, and starlike supramolecular structures are formed at all concentrations, indeed.

Introduction

Dissolution of triblock copolymers in a solvent that selectively dissolves the middle block leads to micellization of the end blocks. A well-known example consists of the polystyrene/polybutadiene/polystyrene (SBS) triblock copolymers.¹ At high concentrations, both polystyrene blocks are part of different micelles, and the polybutadiene block forms a bridge between neighboring micelles, giving rise to the formation of a percolated network (gel). On the other hand, under dilute conditions, the two polystyrene blocks of one polymer chain are aggregated within one micelle, forcing the polybutadiene block to make a loop, so that flowerlike structures are formed. Systems that show very similar behavior include the hydrophobically end-capped urethane-coupled poly(ethylene oxide)s (HEURs)² and telechelic ionomers.³ Especially the HEURs have been studied extensively,⁴ with water as the selective solvent for the PEO block,

forcing the hydrophobic chain ends to aggregate into micelles. These systems show highly interesting rheological properties^{4e,f,5} and are employed as associative thickeners in coatings,^{2b,4a} as sieving media for DNA sequencing,⁶ and as gels for controlled drug release.⁷ The association of the chain ends in these ABA-triblock copolymers is based on phase separation, and the aggregation is a supramolecular process of polymers that have their blocks covalently linked to each other.

Recently, supramolecular polymers have been introduced. There, the repeating units are held together by reversible secondary interactions (e.g., hydrogen bonding, electrostatic interactions, or metal–ligand complexation).⁸ The association of molecules or functional groups is highly directional and specific. This class of supramolecular polymers holds promise

[†] Eindhoven University of Technology.[‡] University of Crete and IESL/FORTH.[§] Max-Planck Institute for Polymer Research.

- (1) (a) Quintana, J. R.; Janez, M. D.; Katime, I. *Polymer* **1998**, *39*, 2111–2117. (b) Villacampa, M.; Quintana, J. R.; Salazar, R.; Katime, I. *Macromolecules* **1995**, *28*, 1025–1031. (c) Hadjichristides, N.; Pispas, S.; Floudas, G. *Block Copolymers*; John Wiley & Sons: New Jersey, 2003. (d) Plestil, J.; Hlavata, D.; Hrouz, J.; Tuzar, Z. *Polymer* **1990**, *31*, 2112–2117. (e) Tuzar, Z.; Konak, C.; Stepanek, P.; Plestil, J.; Kratochvil, P.; Prochazka, K. *Polymer* **1990**, *31*, 2118–2124.
- (2) (a) Kaczmarek, J. P.; Glass, J. E. *Macromolecules* **1993**, *26*, 5149–5156. (b) Glass, J. E. *J. Coat. Technol.* **2001**, *73*, 79–98. (c) Xu, B.; Yekta, A.; Li, L.; Masoumi, Z.; Winnik, M. A. *Colloids Surf.* **1996**, *112*, 239–250.

- (3) Chassenieux, C.; Nicolai, T.; Tassin, J.-F.; Durand, D.; Gohy, J.-F.; Jerome, R. *Macromol. Rapid Commun.* **2001**, *22*, 1216–1232.
- (4) (a) Eglund-Jongewaard, S. K.; Glass, J. E. *Polym. Mater. Sci. Eng.* **1984**, *50*, 485–489. (b) Thibeault, J. C.; Sperry, P. R.; Schaller, E. J. *Polym. Mater. Sci. Eng.* **1984**, *51*, 353–358. (c) Wang, Y.; Winnik, M. A. *Langmuir* **1990**, *6*, 1437–1439. (d) Yekta, A.; Duhamel, J.; Brochard, P.; Adividjaja, H.; Winnik, M. A. *Macromolecules* **1993**, *26*, 1829–1836. (e) Tam, K. C.; Jenkins, R. D.; Winnik, M. A.; Bassett, D. R. *Macromolecules* **1998**, *31*, 4149–4159. (f) Pham, Q. T.; Russel, W. B.; Thibeault, J. C.; Lau, W. *Macromolecules* **1999**, *32*, 5139–5146.
- (5) Ma, S. X.; Cooper, S. L. *Macromolecules* **2002**, *35*, 2024–2029.
- (6) (a) Menchen, S.; Johnson, B.; Winnik, M. A.; Xu, B. *Electrophoresis* **1996**, *17*, 1451–1458. (b) Menchen, S.; Johnson, B.; Winnik, M. A.; Xu, B. *Chem. Mater.* **1996**, *8*, 2205–2208.
- (7) (a) Tae, G.; Kornfield, J. A.; Hubbell, J. A.; Johannsmann, D.; Hogen-Esch, T. E. *Macromolecules* **2001**, *34*, 6409–6419. (b) Tae, G.; Kornfield, J. A.; Hubbell, J. A.; Lal, J. *Macromolecules* **2002**, *35*, 4448–4457.

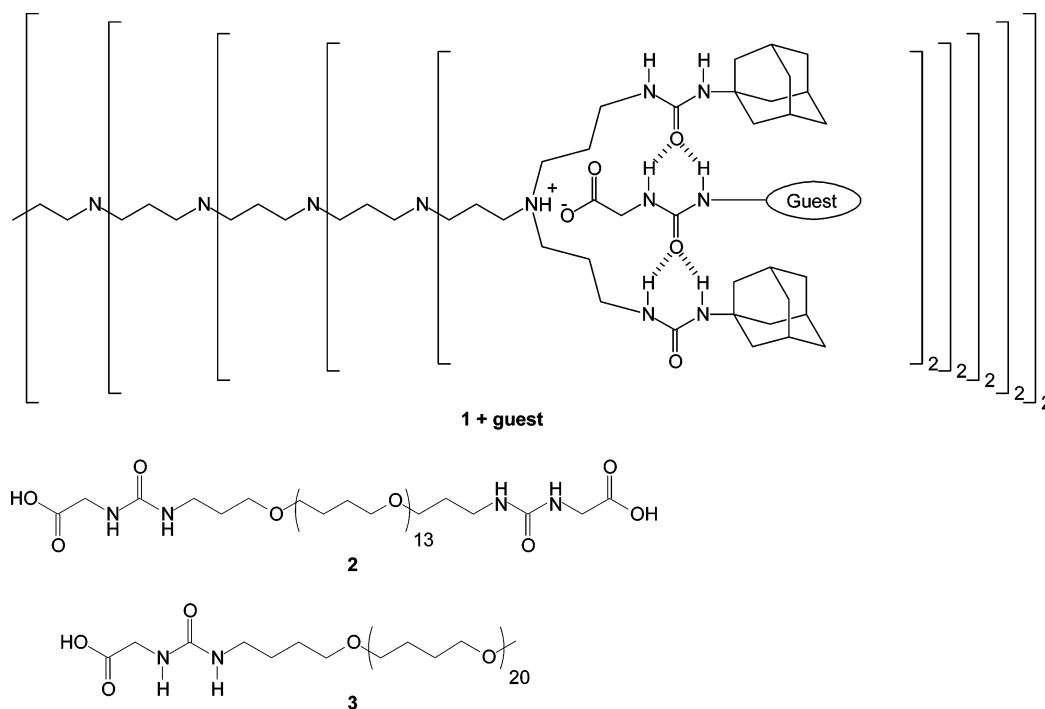


Figure 1. Proposed scheme for the complexation of a dendritic host with a ureido-acetic acid modified guest molecule (**1 + guest**) and the two guest molecules (**2** and **3**) used in this study.

as a unique class of novel materials, because they combine many of the attractive features of conventional macromolecular polymers (mechanical strength) with properties that result from the reversibility of the bonds between the monomer units. Hence, materials are obtained that are able to respond to external stimuli (smart materials) and that are typically in their thermodynamically most stable state. Here, we introduce a new concept of reversible transient networks with two building blocks that are brought together with a directional supramolecular interaction. This concept is based on supramolecular interactions with a dendrimer host, a topic of increasing interest.⁹ We recently introduced a mechanism to modify the periphery of adamantylurea-functionalized poly(propylene imine) dendrimers with guest molecules containing a ureido-acetic acid unit, exhibiting a $K_{\text{ass}} = 10^4 \text{ M}^{-1}$ in chloroform, giving rise to reasonably stable binding (Figure 1).¹⁰ The multivalent dendritic host with 64 end groups complexes 32 guests through strong and directional multiple interactions: both an electrostatic interaction between the protonated tertiary amine and the carboxylate moiety as well as hydrogen bonding between the urea groups of host and guest are proposed to be responsible for this.

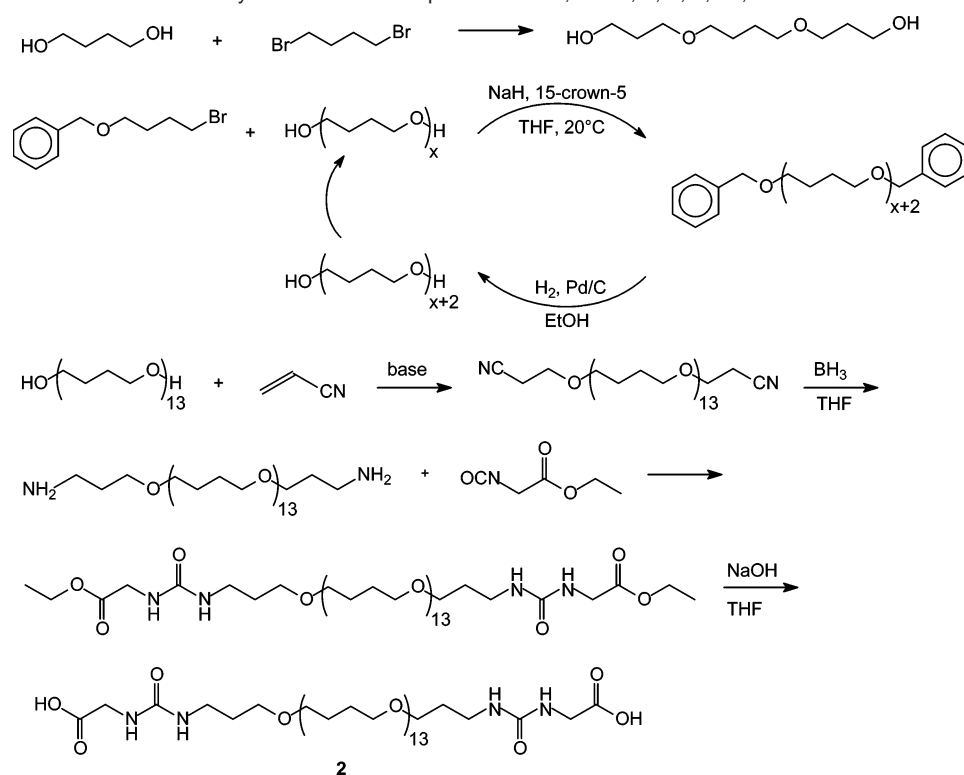
In this paper, we introduce transient supramolecular networks, with reversible, supramolecular interactions between a well-defined number of anchoring points per core (or cross-linking site in the dendritic host) and a macromer with two of these ureido-acetic acid end groups. Both flowerlike structures and transient networks are analyzed in detail by light scattering, showing the presence of an intermediate process of a few (~ 6) connected flowerlike structures.

Design and Synthesis of the Modules

The formation of flowerlike or transient-network structures is based on the reversibility of the interaction between a dendritic core module and a linear chain module. To eliminate the difficulties of polydispersity in the evaluation of the systems under study, we have designed a supramolecular network that consists of truly monodisperse components only. The dendrimer multivalent component, as well as the telechelic oligo(tetrahydrofuran), oligo(THF), are synthesized in a repetitive synthesis. Their properties are investigated with a variety of techniques, and detailed SAXS measurements disclose a number of new features of this novel dynamic system.

The adamantylurea-functionalized poly(propylene imine) dendrimers **1** are synthesized following the reported sequence. To obtain well-defined aggregates, not only the cross-linking core was aimed to be monodisperse, also a new synthesis for oligo(THF) with exactly 13 repeating units and ureido-acetic acid end groups was followed. Scheme 1 shows our synthetic sequence for the synthesis of monodisperse oligo(THF). First, the trimer was prepared by reaction of excess 1,4-butanediol with 1,4-dibromobutane. Benzyl 4-bromobutyl ether was then coupled to this trimer via the Williamson synthesis in THF using 15-crown-5 to enhance the reactivity of the alkoxide formed. An excess of 4-bromobutyl ether was used to compensate for the amount that will be lost due to elimination. After the reaction was completed, the reaction mixture contained next to desired

- (8) (a) Lehn, J.-M. In *Supramolecular Polymers*; Ciferri, A., Ed.; CRC Press: Boca Raton, FL, 2005; pp 3–27. (b) Folmer, B. J. B.; Brunsveld, L.; Meijer, E. W.; Sijbesma, R. P. *Chem. Rev.* **2001**, *101*, 4071–4097. (c) Corbin, P. S.; Zimmerman, S. C. In *Supramolecular Polymers*; Ciferri, A., Ed.; CRC Press: Boca Raton, FL, 2005; pp 153–185. (d) Schubert, U. S.; Eschbaumer, C. *Angew. Chem., Int. Ed.* **2002**, *41*, 2892–2926.
- (9) (a) Zimmerman, S. C.; Zeng, F.; Reichert, D. E. C.; Kolotuchin, S. V. *Science* **1996**, *271*, 1095–1098. (b) Daniel, M.-C.; Ruiz, J.; Astruc, D. *J. Am. Chem. Soc.* **2003**, *125*, 1150–1151. (c) Hirst, A. R.; Smith, D. K.; Feiters, M. C.; Geurts, H. P. M. *Langmuir* **2004**, *20*, 7070–7077.
- (10) (a) Baars, M. W. P. L.; Karlsson, A. J.; Sorokin, V.; de Waal, B. F. W.; Meijer, E. W. *Angew. Chem., Int. Ed.* **2000**, *39*, 4262–4265. (b) Boas, U.; Karlsson, A. J.; de Waal, B. F. M.; Meijer, E. W. *J. Org. Chem.* **2001**, *66*, 2136–2145. (c) Boas, U.; Sontjens, S. H. M.; Jensen, K. J.; Christensen, J. B.; Meijer, E. W. *ChemBioChem* **2002**, *3*, 433–439. (d) Baars, M. W. P. L.; Meijer, E. W. *Polym. Mater. Sci. Eng.* **1997**, *77*, 149–150. (e) Broeren, M. A. C.; de Waal, B. F. M.; van Genderen, M. H. P.; Sanders, H. M. H. F.; Fytas, G.; Meijer, E. W. *J. Am. Chem. Soc.* **2005**, *127*, 10334–10343.

Scheme 1. The Synthetic Scheme for the Synthesis of Monodisperse Guest **2**, $x = 3, 5, 7, 9, 11,$ and 13 

product also the excess of reagent and elimination products. Subsequently, the benzyl groups of all products in the reaction mixture were cleaved by hydrogenation. In this reaction, the double bonds of the elimination products were hydrogenated as well. After the new byproduct 4-bromo-1-butanol was converted to THF by cyclization at alkaline conditions, all byproducts were easily removed by evaporation. The pentameric oligo(THF) product with two more units than the starting trimer was subsequently purified by crystallization. The same sequence was used to obtain the heptamer, nonamer, undecamer, and finally the tridecamer. All oligomers were pure on SEC and NMR. Similar to dendrimers, mass spectrometry is unique in analyzing the exact structural purity. The MALDI-TOF spectrum of the tridecamer showed a polydispersity of 1.004; this is quite similar to the 1.002 for the fifth generation dendrimer. The tridecamer was transformed into guest molecule **2** (Scheme 1) by a double Michael addition with acrylonitrile, followed by reduction with BH_3 in THF to afford the bis-amine. Pure **2** was obtained after both amine end groups were reacted with ethyl isocyanatoacetate followed by careful hydrolysis to prevent hydantoin formation. The molecular weight of the module used in this study is 1270 g/mol.

Monofunctional oligo(THF) guest **3** was prepared as a reference compound starting with a living cationic ring-opening polymerization of THF followed by end-group modification similar to the procedure of **2**. Product **3** was well soluble in chloroform and was successfully characterized by 1H NMR and FT-IR. Due to some fractionation of the polymer during workup, the number-averaged molecular weight was finally 1650 g/mol.

Molecular Characterization of the Supramolecular Complex

Several techniques have been used to study the molecular structure of the guest–host system consisting of guests with

the ureido-acetic acid unit and a host of a adamantylurea functionalized poly(propylene imine) dendrimer of the fifth generation: for example, 1H NMR, FT-IR, isothermal microcalorimetry, and NOESY NMR.^{10a} Two solutions (between 30 and 100 mg/mL) in chloroform were prepared, the first containing the dendritic host **1** and the second containing the bifunctional guest **2**. 1H NMR and FT-IR spectra were taken of these solutions. Subsequently, the two solutions were mixed in a 1:16 molar ratio, making sure that a stoichiometric ratio of both complexing groups was achieved. The solution remained completely clear and homogeneous, and an increase of the viscosity was observed. Again, 1H NMR and FT-IR spectra were taken of this solution and compared with the spectra of the host and guest solutions. The effect of complexation is evident from the FT-IR spectrum in the carbonyl region ($1800–1600\text{ cm}^{-1}$). Upon complexation, the 1732 cm^{-1} band of the acid disappears due to protonation of the tertiary amine of the dendrimer. The urea bands of guest **2** (at 1664 cm^{-1}) and host **1** (1637 cm^{-1}) both move to 1630 cm^{-1} in agreement with a strong hydrogen-bonded state in the complex. Even the host shows an increase in hydrogen bonding upon complexation.¹¹ No shifts in the infrared spectra are observed upon diluting the solution, demonstrating the robustness of the supramolecular complex.

1H NMR spectra of bifunctional guest, host, and complex show features typical for the kind of interactions indicated in Figure 1. Upon addition of the guest to the host, the peak at 2.4 ppm, corresponding to the methylene groups adjacent to tertiary amines of the host, broadens considerably and shifts slightly downfield. This is caused by protonation of these tertiary amines by the carboxylic acid functionalities of the guest. Furthermore, the peaks between 5.4 and 6.2 ppm, corresponding to the urea groups of both host and guest, shift slightly downfield

(11) Baars, M. W. P. L.; Meijer, E. W. *Polym. Mater. Sci. Eng.* **1997**, *77*, 149–150.

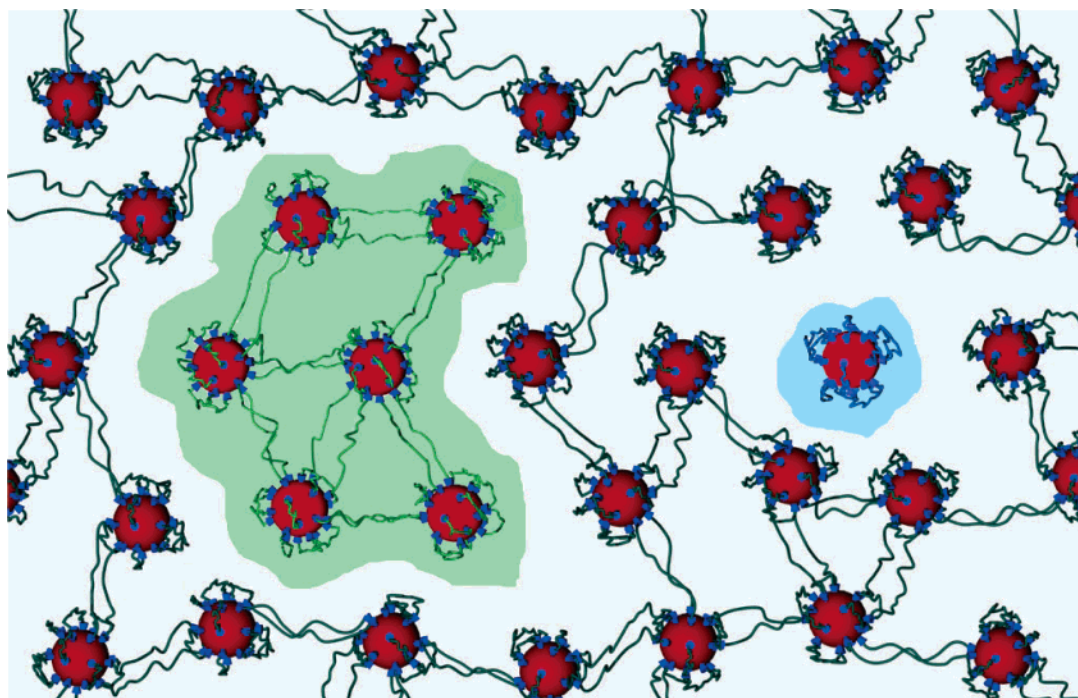


Figure 2. Schematic illustration of the supramolecular complexes, ranging from flowerlike structures (blue area), via the aggregates of flowerlike structures (green area), to the supramolecular transient network (gray area).

and broaden as well. This is an indication that hydrogen bonding between the dendritic host and the encapsulated guest is taking place. The broadening is the result of the rigidification of the periphery at the site of hydrogen bonding and of an increase in (apparent) molecular weight upon complexation.

The availability of designed stations in the dendritic host and the directionality of the host–guest interactions is the basis of the proposed supramolecular complex of Figure 2, which is explained below. Although molecular spectroscopic tools are all in agreement with the supramolecular structures in dilute solutions, a confirmation of the mechanism and the emerged supramolecular structures at dense conditions is needed. A stoichiometrically 1:16 complex of the supramolecular system with the monodisperse dendrimer **1** and the monodisperse guest **2** (in dilute solutions of $c < 20$ g/L) is revealed by its molecular mass determined by dynamic light scattering (see below). With increasing concentration, the inherently oligomeric nature of the supramolecular complex is anticipated to fold into intermediate larger structures, which eventually drive the solution into a transient transparent supramolecular network (Figure 2). A proper characterization of this dynamic system over the full concentration range, being a challenging task, is described below.

The Dynamics of the Supramolecular Structures

We employed photon correlation spectroscopy, a laser light scattering technique operating in the 10^{-7} – 10^3 s range, to probe the dynamics of the guest–host structures in solution over a broad range of concentrations. The amplitude and the time scale of the fluctuations in the intensity of the scattered light (due to the thermal molecular motion) characterize the scattering moieties. In the absence of thermodynamic interactions at low concentrations, the measured intensity autocorrelation function yields the dynamic form factor $C(q,t) = P(q) \exp(-D_0 q^2 t)$ at different wave vectors q in the range 5×10^{-3} to 0.034 nm $^{-1}$.

This corresponds to probing lengths of 180–1200 nm using this technique.

From the single translational diffusion coefficient $D_0 = k_T T / (6\pi\eta_s R_h)$ (k_T is the Boltzmann's constant, T is the absolute temperature, and η_s is the solvent viscosity) of the 1:16 guest–host complex at dilute concentrations (< 3 g/L), the computed hydrodynamic size of $R_h = 3.7$ nm is determined. This R_h of the complex exceeds the corresponding size (2.4 nm) of the bare dendritic host and is smaller than the 1:32 complex of **1** and **3**, exhibiting a computed hydrodynamic size of $R_h = 4.0$ nm. As expected from the size ($qR_h < 1$) of the complexes, the time average intensity $P(q)$ is found to be independent of q . From the experimental $P(0)$ and the refractive index contrast ($dn/dc = 0.070$ cm 3 /g in chloroform), the obtained molecular mass M of the complex of **1** and **2** amounts to 36.5 ± 1 kg/mol, being very close to the proposed ideal 1:16 supramolecular flowerlike structure, which is calculated to be 38.8 kg/mol. Note that the solution of the bare host in chloroform exhibits a different value for $dn/dc = 0.103$ cm 3 /g, supporting a surface modification of the dendritic host.

A complex is therefore formed via stoichiometric mixing (1:16) host and guest with a flowerlike structure that is well represented by Figure 2 (blue area). This type of effectively grafted particle is distinct from the one-component triblock copolymer micelles. Hence, the primary structure in the dilute regime should be rather robust as indicated by the constant R_h up to the boiling temperature of the solvent, that is, 61 °C. In fact, D_0 displays an activation energy $E_A = 1.6$ kcal/mol that is similar to solvent viscosity. Yet, the designed new supramolecular structure exhibits distinct material properties when it is transformed into a network (see below).

To appreciate the revealed structural and dynamic changes in nondilute solutions, we investigated the behavior of the individual partners, host, and guest molecules as well and

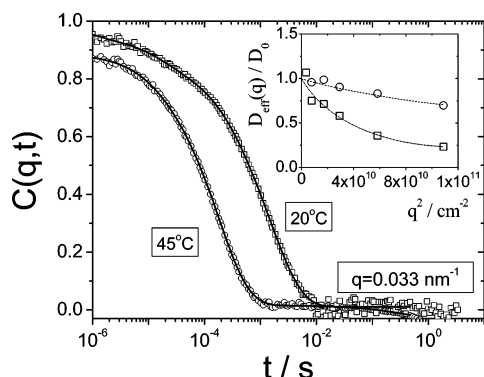


Figure 3. Dynamic structure factor $C(q,t)$ of the 1:16 stoichiometric mixture of the dendritic host and monodisperse telechelic guest for 71 g/L in chloroform at a given probing length (~ 190 nm) and the two indicated temperatures. The solid lines indicate a bimodal distribution function fit to $C(q,t)$. Inset: Normalized $D_{\text{eff}}(q)/D(0)$ for the slow process of $C(q,t)$, using $D(0) = 2.95 \times 10^{-8}$ (20 °C) and 8.25×10^{-8} cm²/s (45 °C). The dotted lines represent the polynomial fit discussed in the text.

summarize it here. As expected,¹² the dendritic host without guest behaves like a hard particle up to the overlap concentration $c^* = M/(N_A v) \approx 500$ g/L (N_A is the Avogadro number, and $v = (4/3)\pi R_h^3$ is the volume of the dendrimer). Furthermore, it forms an ideal solution in chloroform, that is, the interaction parameter $A_2 \approx 0$. Above this concentration, first clusters are formed and then the solution vitrifies above about 800 g/L at room temperature. On the other hand, the monodisperse telechelic guest alone exhibits unfavorable solute–solvent interactions ($A_2 < 0$) in the same solvent, and hence aggregates are observed at lower concentrations ($c \approx 100$ g/L) due to H-bonding chain association. The solution remains in the (highly viscous) liquid state for concentrations as high as 95 wt %.

The flowerlike complex exhibits a very narrow dilute regime ($c < c' \approx 20$ g/L) with unfavorable ($A_2 < 0$) solute–solvent interactions as the result of its coated structure (Figure 2, blue area). This finding is surprising given its nanometer size with an anticipated broad dilute regime (estimated $c^* = 300$ g/L). Above this transition concentration c' , the dynamic structure factor $C(q,t)$ changes from the single-exponential shape in the dilute regime to a complex shape revealing a crossover to a second regime. Figure 3 shows the $C(q,t)$ of the 1:16 supramolecular complex at 71 g/L for two temperatures at a constant $q (=0.033 \text{ nm}^{-1})$, which corresponds to a diffusion length of 190 nm. The broad two-step-decay shape of $C(q,t)$ at 20 °C extending over four decades in time is best represented by a bimodal distribution of relaxation times obtained by standard analysis,¹³ which yields the rate $\Gamma_i(q)$ and the intensity $I_i(q)$ of the i -th ($i = f, s$) process at a given q . The fast process with $\Gamma_f = D_f q^2$ and q -independent intensity I_f resembles the single-exponential process in the dilute regime and is therefore assigned to the diffusion of the flowerlike structures; in fact, $D_f \approx D_0$.

For the new second process, unexpected at these very low concentrations, I_s is also q -independent, compatible with sizes less than about 20 nm, but the relaxation rate Γ_s shows a peculiar q -dependence. Unlike D_f , the slower effective $D_{\text{eff}} \equiv \Gamma_s/q^2$ is not a constant but is found to decrease with increasing q . This

counterintuitive slower diffusion at short distances than at long distances, as shown in the normalized $D_{\text{eff}}(q)/D(q=0)$ versus q plot in the inset of Figure 3 for two temperatures, is rarely observed.¹⁴ Triggered by a theoretical analysis¹⁵ of rigid rod diffusion at concentrations near the lyotropic transition, we have parametrized this variation (intermediate between q^2 and q^0) by $D_{\text{eff}}(q) = D(0)(1 + Bq^2 + B'q^4)$ (dotted line in the inset of Figure 3). The negative value of the dynamic virial coefficient $B (< 0)$ reflects short-range driving forces in contrast to the common osmotic pressure measured in the low- q macroscopic limit. This might arise from attractive local interactions between the primary rigid guest–host structures (blue area in Figure 2).

This unusual behavior can be rationalized if we realize that above about c' (~ 20 – 25 g/L) the average distance between the supramolecular complex matches the contour length (~ 14 nm) of the monodisperse guest. Hence, a secondary structure (Figure 2 green area) via bridging of the primary flowerlike structures is feasible. Based on the moderate activation energy $E_A \approx 6$ kcal/mol obtained from the temperature dependence of $D_{\text{eff}}(q=0)$, this guest–host exchange occurs very fast so that the effective diffusion describes the translational motion of this quasi-supramolecular assembly. The latter consists of about six primary objects as obtained from the comparison of the corresponding intensities I_s/c and $I(c=0)/c$. The slower motion at high q 's, ascribed¹⁵ to the distance-dependent interactions (Bq^2), apparently reflects delayed internal rearrangements of the secondary structure. This assembly undergoes diffusive translation at long distances and long times as compared to the motion of the single bulk particle of the same size. However, when this assembly is probed at short distances and respective short times, it exhibits a slowing down. This new finding reflects interactions between the constituent (~ 6) primary objects, bringing analogies to cage dynamics.¹⁶

Because the second process in $C(q,t)$, associated with the secondary dynamic structure, is absent in the dendrimer solution, it is reasonable to relate it with the bridging of the flowerlike structure through the supramolecular interactions, and hence temperature should matter. As shown in the inset of Figure 3, the pertinent variation $D_{\text{eff}}(q)$ at 45 °C is clearly weaker described by $B(45 \text{ °C}) \approx 1/6 B(20 \text{ °C})$. Further, the reduction of the intensity I_s for the slow process at 45 °C suggests a decrease for the population of the interconnected flowerlike structures (Figure 2, green area). With increasing concentration at ambient temperatures, the solution of the supramolecular guest–host complex should undergo an additional transformation to a transient network as sketched in Figure 2 (gray area).

Indeed, above another transition concentration of about $c'' = 100$ g/L, the dynamic structure factor $C(q,t)$ of Figure 4a displays a third slower mode associated with big clusters, evident from the strong q -dependent intensity (Figure 4a). The displayed characteristics of the ergodic (i.e., nontrapped configurations) $C(q,t)$ are typical for weak gellike systems.¹⁷ This notion is further corroborated by the strong increase of the solution viscosity and the activation energy $E_A \approx 18$ kcal/mol of the respective slow diffusion. The nature of these transient assemblies can be further elucidated by means of linear rheological

(12) Topp, A.; Bauer, B. J.; Prosa, T. J.; Scherrenberg, R.; Amis, E. J. *Macromolecules* **1999**, *32*, 8923–8931.

(13) Fytas, G. In *Light scattering from dense polymer systems. Scattering Encyclopedia*; Pike, P., Sabatier, P., Eds.; Academic Press: New York, 2003; Vol. 35, Chapter 2, pp 849–863.

(14) Delong, M.; Russo, S. P. *Macromolecules* **1991**, *24*, 6139–6155.

(15) Doi, M.; Shimada, T.; Okano, K. *J. Chem. Phys.* **1988**, *88*, 4070–4074.

(16) Segre, P. N.; Pusey, P. N. *Phys. Rev. Lett.* **1996**, *77*, 771–774.

(17) Kapnistos, M.; Vlassopoulos, D.; Fytas, G.; Mortensen, K.; Fleischer, G.; Roovers, J. *Phys. Rev. Lett.* **2000**, *85*, 4072–4075.

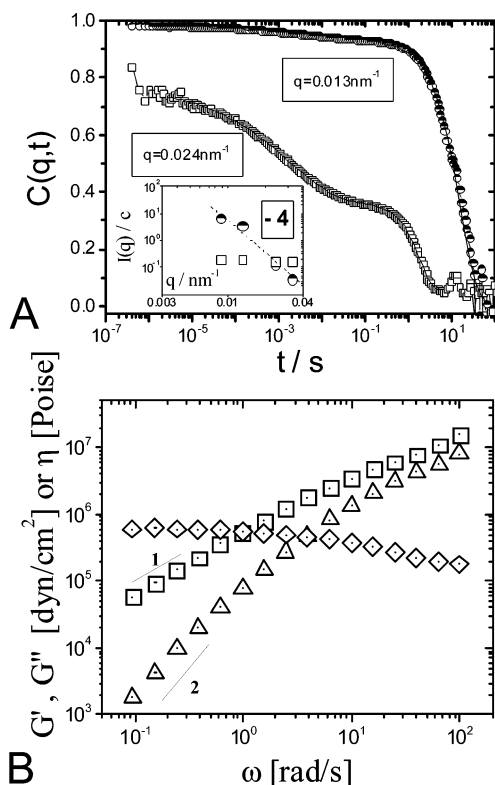


Figure 4. (a) Dynamic structure factor of the 1:16 stoichiometric host–guest mixture at 128 g/L, 20 °C, and two magnifications given by the values of q . Inset: The intensity $I(q)$ for the intermediate and slow process. The dashed line has a slope -4 . (b) Dynamic shear moduli G' (Δ), G'' (\square), and the complex viscosity (\diamond) as a function of the deformation frequency for the same system at a concentration of about 90 wt % at ambient temperatures. The solid lines indicate the limiting scaling laws for flow.

measurements. The dynamic shear moduli are shown in Figure 4b for a concentration of about 90 wt %. Both the elastic (G') and the viscous (G'') moduli at low frequencies have reached the limiting flow scaling relations against frequency, 2 and 1, respectively, whereas the zero shear viscosity, η , has achieved high ($\sim 6 \times 10^5$ Poises) values. Based on these rheological data and the existence of big clusters manifested in Figure 4a, it is evident that there is no permanent interconnected percolated network, which would preclude flow yielding frequency independent $G' > G''$. Instead, the high η can be rationalized by the presence and ergodic response of the big clusters, which can slide against each other, allowing for slow flow. The lack of a plateau in G' is also compatible with this proposed structure of Figure 2, because the short chain guests are unentangled.

Evaporation of the solution to complete dryness gave a transparent film with a completely different appearance than the starting host and guest, which are an amorphous powder and a waxy solid, respectively. The film possesses appealing mechanical properties, such as elasticity, although it is slightly sticky.

The Three Supramolecular Structures

The physical state of the solution is mapped in the “phase diagram” given in terms of the total I/c (Figure 5a) and $D_i(q = 0)$ (Figure 5b) of the various processes versus the supramolecular complex concentration at 20 °C. Three regimes are consistently revealed in both plots. Dilute regime I is characterized by the single process for the flowerlike complex (Figure 2), having

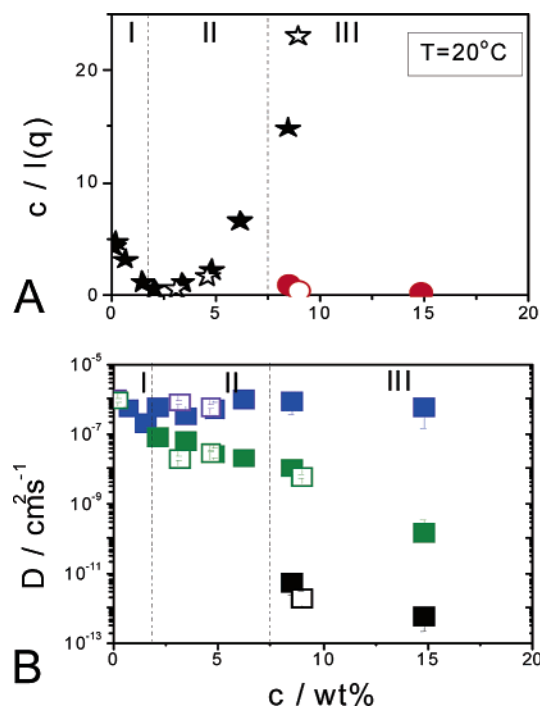


Figure 5. “Phase state diagram” in terms of the total reduced intensity c/I (*) in (a) and the diffusion constant D in (b) for the three revealed structures versus the concentration c of the 1:16 complex at 20 °C. Regions I, II, and III indicate the three different regimes. In (a), the circles are for the slow gellike process at $q = 8.5 \times 10^{-3} \text{ nm}^{-1}$, and in (a) and (b), the open symbols refer to the complex formed at $c = 48 \text{ g/L}$ ($>c'$). In (b), the colors of the symbols correspond to the areas of Figure 2.

unfavorable interactions reflected in the decrease of c/I and $D(c)$. The crossover into regime II is marked by the turn-over in the c -dependence of c/I and the bifurcation of $D(c)$ due to the coexistence of the primary and secondary supramolecular objects. With increasing crowding, the solution becomes more homogeneous with weaker fluctuations (I/c decreases) via the overlap of the interconnected complexes, and progressively the solution becomes more viscous. Regime II extends up to $c'' \approx 100 \text{ g/L}$ marked by the appearance of a third slow mode in regime III related to the formation of big clusters arranged in a loose network-like fashion (Figure 5). It is remarkable that all three structures of Figure 2 are present in regime III and the primary flowerlike supramolecular complex keeps its initial fast diffusion coefficient. The presence of the flowerlike complexes even at very high concentration is similar to the presence of cyclic structures in linear polymers (e.g., ring-chain equilibrium in Nylon-6 and caprolactam) and suggests equilibrium of large and small supramolecular objects.¹⁷ The strong increase of the viscosity, primarily attributed to the slow process, precludes dynamic light scattering measurements at even higher concentrations. It is worth mentioning that telechelic macro-ionomers lacking the present directional interactions show polymer-like cooperative diffusion driven by osmotic pressure and an ill-defined gellike process.³

The stability of the physical state of the 1:16 stoichiometric host–guest mixture was examined by preparing two different initial concentrations at 3.2 g/L ($<c'$) and 48 g/L ($>c'$ and $<c''$) to create higher concentrations by slow solvent evaporation indicated by open and solid symbols in Figure 5. Despite the possibility of thermodynamic metastability when the stoichiometric host–guest mixing occurs at $c > c'$, the two experimental

protocols lead to similar structures, unique for this system designed. Alternatively, a stoichiometric mixture (1:32) of the same dendrimer with chemically similar but mono-functional guest **3** in chloroform behaves distinctly different, for example, low viscosity, and moreover phase separates above 120 g/L at 20 °C.

Conclusions and Outlook

A new approach has been presented to create flowerlike and transient supramolecular network structures. In contrast to the block-copolymers studied so far, the two physically different blocks are held together by supramolecular secondary interactions that are highly directional and reversible. This allows the dynamic system to be under thermodynamic equilibrium. The association constant of the supramolecular binding of about $K_{\text{ass}} = 10^3\text{--}10^4 \text{ M}^{-1}$ gives rise to a reasonable stable binding between the two components, while at the same time the reversible nature is ensured. The dendritic structure of the cross-linking unit or multivalent associate creates the additional stability of the supramolecular complexes formed. The monodisperse character, as a result of unique synthetic pathways, of both components allows detailed analysis, and dynamic light scattering has been used to elucidate the different supramolecular structures formed. The observed collective process of roughly six flowerlike structures exhibits unique temperature dependence. The resulting phase state in a range of concentrations from the dilute up to the melt reveals strong interactions well below the nominal overlapping concentration and a highly viscous fluid that does not bear permanent network feature.

With this new approach of supramolecularly bringing together components that can form well-defined superstructures, a new avenue is created. It is anticipated that it should be possible to perform this approach in water and that some of the supramolecular units of the dendrimer can be used to anchor (bio-)functional units.

Experimental Section

The synthesis and characterization of the materials used are given in the Supporting Information.

Photon Correlation Spectroscopy (PCS). The solution of dendrimer in CHCl_3 (amylene stabilized) at a concentration of 3.2 g/L was filtered through a 1 μm Teflon Millipore filter into the dust free optical cell (i.d. 8 mm). The guest/ CHCl_3 solution at the desired stoichiometric composition was then filtered into the dendritic host solution in the light scattering cell. Preparation of higher concentrations was accomplished by slow solvent evaporation. The desired dynamic structure factor $C(q,t) = [(G(q,t) - 1)/f^*]$ was computed from the measured light scattering intensity $I_s(q,t)$ (using ALV5000 digital correlation) and the autocorrelation function $G(q,t)$ over a broad time range (0.1 μs to 100 s) at a given scattering wave vector $|\mathbf{q}| = (4\pi n/\lambda) \sin(\theta/2)$, where n , λ , and θ are the refractive index of the medium, laser wavelength in a vacuum, and scattering angle, respectively, and f^* is an instrumental contrast factor; q varies between (0.004–0.034) nm^{-1} . The amplitude α of $C(q,t)$ at short times ($<0.1 \mu\text{s}$) yields the intensity $I(q) = \alpha I_s(q)$ associated with the individual moieties, that is, complex or their interactions in nondilute solutions. Further, the origin of the $C(q,t)$ is reflected in its temporal decay at a given q . In the absence of interactions (dilute solutions), its exponential decay rate $\Gamma(q) = Dq^2$ relates to the translational diffusion coefficient D of the probed species and hence their hydrodynamic size. In the latter case, $I(q=0)$ yields the molecular weight of the diffusing object.

Acknowledgment. We are grateful to Mr. Bas de Waal (TU/e) and Mrs. Antje Larsen (FORTH) for technical assistance, and we acknowledge the financial support of the EU (HPRN-CT-2000-2003) and the Council for Chemical Sciences of The Netherlands Organization for Scientific Research (CW-NWO).

Supporting Information Available: Additional information about the synthesis and characterization of the molecules used. This material is available free of charge via the Internet at <http://pubs.acs.org>.

JA051775G